AMMRC TR 79-48

LEVEL II

AD

(12)

AD A078275

CHARACTERISTICS OF MECHANICALLY FASTENED JOINTS OF CIP/HIP-1 BERYLLIUM

DDC
RECEIVED
DEC 17 1979
E

SHUN-CHIN CHOU, JAMES H. RAINEY, and RONALD A. SWANSON
BALLISTIC MISSILE DEFENSE MATERIALS PROGRAM OFFICE

DDC FILE COPY

August 1979

Approved for public release; distribution unlimited.

ARMY MATERIALS AND MECHANICS RESEARCH CENTER
Watertown, Massachusetts 02172

79 12 14 051

The findings in this report are not to be construed as an official Department of the Army position, unless so designated by other authorized documents.

Mention of any trade names or manufacturers in this report shall not be construed as advertising nor as an official indorsement or approval of such products or companies by the United States Government.

DISPOSITION INSTRUCTIONS

Destroy this report when it is no longer needed.
Do not return it to the originator.

REPORT DOCUMENTATION PAGE		READ INSTRUCTIONS BEFORE COMPLETING FORM
1. REPORT NUMBER AMMRC-TR-79-48	2. GOVT ACCESSION NO.	3. RECIPIENT'S CATALOG NUMBER
4. TITLE (and Subtitle) CHARACTERISTICS OF MECHANICALLY FASTENED JOINTS OF CIP/HIP-1 BERYLLIUM		5. TYPE OF REPORT & PERIOD COVERED Final Report 6. PERFORMING ORG. REPORT NUMBER
7. AUTHOR(s) Shun-Chin Chou, James H. Rainey, and Ronald A. Swanson		8. CONTRACT OR GRANT NUMBER(s)
9. PERFORMING ORGANIZATION NAME AND ADDRESS Army Materials and Mechanics Research Center Watertown, Massachusetts 02172 DRXMR-H		10. PROGRAM ELEMENT, PROJECT, TASK AREA & WORK UNIT NUMBERS D/A Project: 8X363304D215 AMCMS Code: 633304.21500.03
11. CONTROLLING OFFICE NAME AND ADDRESS U. S. Army Materiel Development and Readiness Command, Alexandria, Virginia 22333		12. REPORT DATE August 1979 13. NUMBER OF PAGES 31
14. MONITORING AGENCY NAME & ADDRESS (if different from Controlling Office) 12 37		15. SECURITY CLASS. (of this report) Unclassified 15a. DECLASSIFICATION/DOWNGRADING SCHEDULE

16. DISTRIBUTION STATEMENT (of this Report)

Approved for public release; distribution unlimited.

17. DISTRIBUTION STATEMENT (of the abstract entered in Block 20, if different from Report)

18. SUPPLEMENTARY NOTES

19. KEY WORDS (Continue on reverse side if necessary and identify by block number)

Beryllium	Bolted joints
Bearing strength	Mechanical tests
Loading rate	Stress analysis

20. ABSTRACT (Continue on reverse side if necessary and identify by block number)

(SEE REVERSE SIDE)

Block No. 20

ABSTRACT

Mechanically fastened joints of CIP/HIP-1 beryllium were investigated. A standard ASTM pin-jointed bearing strength test was used to determine the effect of hole size and edge distance-to-thickness ratios on the bearing strength of beryllium plates. Joints for structures were studied by testing two types of arrangements of pin holes with different transverse pitches.

From the standard ASTM pin-jointed bearing strength tests, it was determined that the design criterion for single-pinned joints of CIP/HIP-1 beryllium should be based on maximum stress instead of net cross-section stress. Furthermore, it was found that if the edge distance-to-pin diameter ratio was kept constant, the specimens would have the same bearing yield stress, bearing strength, and maximum bearing strain. In the investigation of structural bolted joints, the double-bolted joints show that the transverse pitch and hole pattern have no effect on the load-carrying capability.

CONTENTS

Accession For
NTIS GRA&I
DDC TAB
Unannounced
Justification
By
Distribution/
Availability Codes
Dist | Avail and/or special
A

I. INTRODUCTION

The application of beryllium for potential use in aerospace structures has been limited because of poor ductility. CIP/HIP-1 beryllium from Kawecki Berylco, Inc., exhibits a ductility of greater than 3% in uniaxial tension. Combining this increase in ductility with the high specific modulus, 6×10^8 in. (15.2×10^8 cm), makes beryllium a serious candidate along with the advanced composites as strategic missile structural materials. Hence, an extensive characterization program on CIP/HIP-1 beryllium has been completed. This characterization includes determination of stress-strain behavior over a wide range of strain rates, temperature effects, Bauschinger effect, yield surface and strength under biaxial loadings, and fracture toughness. Early program results have been reported in References 1 and 2 and the remaining results will be reported in the future.

This study deals with the important question to missile designers: Can beryllium structures be connected together by mechanically fastened joints? The response to this need was to conduct a two-stage test program. In the first stage, a standard (ASTM-E-238) pin-jointed bearing strength test was performed to evaluate load-carrying capability of a single-pin-loaded specimen and provide the basic design data for mechanical fastened joints. In the second stage, test specimens with three types of pinhole arrangements were tested to evaluate the effect of pitch on the load-carrying capability and determine the geometric parameters of the multiple hole structural joints.

II. MATERIAL

Material description for CIP/HIP-1 beryllium is given in detail in References 1 and 2. To make this a self-contained report, a brief description is given. All specimens were taken from a hollow CIP/HIP-1 beryllium cylinder with a wall thickness of three inches. The cylinder was fabricated by first cold isostatically pressing impact-attritioned P-1 powder at 60,000 psi (414 MPa) at 75% of theoretical density. This was followed by hot isostatic pressing in evacuated steel cans fitted with steel mandrels. The assemblies were outgassed at 1350 F (730 C) and isostatically pressed for three hours at 1950 F (1065 C) at a pressure of 15,000 psi (103 MPa).

Density of the finished pressing was 1.852 g/cc. Grain size ranged from 8 to 9 microns, and the chemical analysis shows that the material contains

Wt. %	Parts Per Million											
BeO	Fe	Al	Mg	Si	C	Cr	Co	Cu	Pb	Mn	Mo	Ni
1.09	200	40	35	83	230	25	<5	40	1	13	<10	125

1. CHOU, S. C., ARONIN, L. R., DIGNAM, J. F., and RAINEY, J. H. *Mechanical Behavior of CIP/HIP-1 Beryllium as a Function of Strain Rate and Stress History.* Proceedings of the Fourth International Conference on Beryllium, London, England, 4-7 October 1977.
2. DIGNAM, J. F., ARONIN, L. R., CHOU, S. C., and RAINEY, J. H. *Temperature Effects on Mechanical Properties of CIP/HIP-1 Beryllium.* Proceedings of the Fourth International Conference on Beryllium, London, England, 4-7 October 1977.

Most specimens taken from the pressed hollow cylinder for the purpose of this study were machined in such a way that the direction of load for specimens would always be along the longitudinal axis of the hollow cylinder (see Figure 1), except five specimens for which the load direction would be along the circumferential direction of the cylinder. This arrangement would evaluate the isotropy of the material.

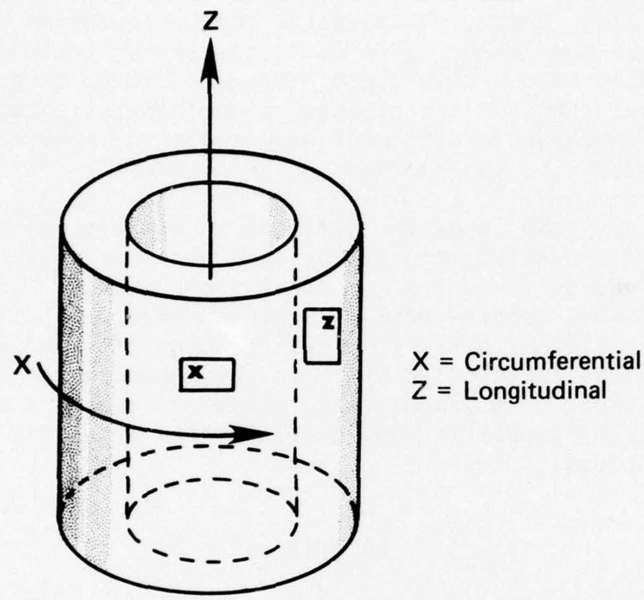

Figure 1. Orientation of specimens machined from CIP/HIP-1 beryllium cylinder in the X and Z directions.

III. PIN-TYPE BEARING TESTS (ASTM-E-238)

Pin-type bearing yield and strength data are important because they establish baseline bearing data values from which mechanically fastened joints can be designed. The objectives of the pin-type bearing tests of this study are to determine the effects of geometry, strain rate, directionality, and specimen thickness on the bearing yield and bearing strength of CIP/HIP-1 beryllium. The tests were performed according to ASTM Standard E-238 by using an automated material characterization system. This system is described in detail in the Appendix.

Specimen Configuration

According to ASTM Standard E-238, the specimen shall be a flat sheet type, with the full thickness of the product being used, if possible. A ratio of pin diameter to specimen thickness of from 2 to 4 has been used to prevent breaking or bending the pin before the bearing strength is obtained. If a specimen is too thin, buckling may occur. The hole should have approximately the same diameter as for the intended use. The width of the specimen should be about 4 to 8 times the hole diameter. The ratio of edge distance to hole diameter of 1.5 and 2.0 is commonly used. The total length of the test specimen is not critical.

Based on these guidelines, the dimensions of specimens used in this study are listed in Figure 2. Two specimen thicknesses (T) were chosen, namely: 0.3 inch (0.762 cm) and 0.25 inch (0.635 cm); and two hole diameters (D) 0.625 inch (1.588 cm) and 0.5 inch (1.27 cm) were used to determine the bearing strength of the specimen. Both ratios of edge distance (E) to hole diameter of 1.5 and 2.0 were used to investigate the effect of the ratio on the bearing strength. In other words, there are four groups of specimens used in the pin-type bearing test to determine the bearing characteristics.

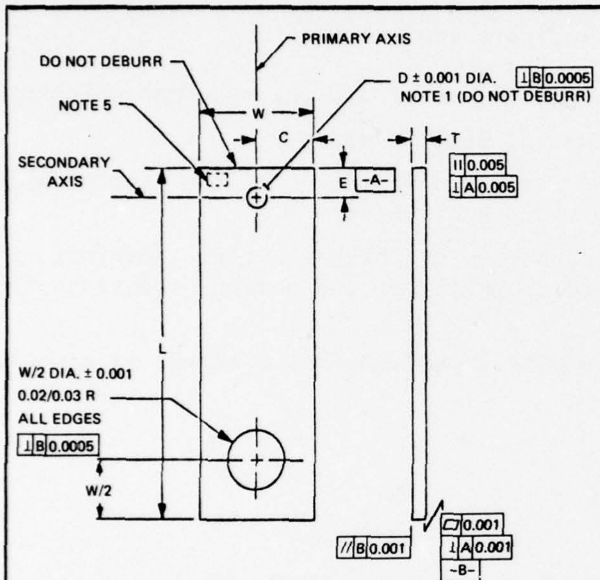

GROUP NO.	T	W	E	D	L	C
-01	0.300	3.000	0.938	0.625	6.000	1.500
-02	0.300	3.000	1.250	0.625	6.000	1.500
-03	0.250	3.000	0.750	0.500	6.000	1.500
-04	0.250	3.000	1.000	0.500	6.000	1.500

1. A SMOOTH, ROUND HOLE WITH A MINIMUM OF COLD WORK ON THE SURFACE MUST BE OBTAINED. THE FINISHED HOLE IS GENERALLY BORED, REAMED, OR GROUND AS A FINAL OPERATION TO OBTAIN THE DESIRED DEGREE OF ROUNDNESS. ANY BURR ON THE PERIPHERY OF THE HOLE IS INDICATIVE OF A COLD WORKED SURFACE ON THE HOLE AND SHOULD BE AVOIDED. REMOVAL OF THE BURR WILL NOT ELIMINATE THE COLD WORK. REF. ASTM E 238-68.
2. UNLESS OTHERSIWE SPECIFIED, ALL SURFACES TO HAVE A 32μ.
3. BREAK OUTSIDE EDGES APPROXIMATELY 0.03 RAD. UNLESS SPECIFIED.
4. FOR BERYLLIUM ONLY: ETCH TO FINISHED DIMENSIONS.
5. MARK IN 1/8" CHARACTERS WITH BLACK EPOXY INK, OR ELECTRO ETCH, APPLICABLE SPECIMEN IDENTIFICATION NUMBER.

UNLESS OTHERWISE SPECIFIED DIMENSIONS *ARE IN INCHES AND SHALL FALL WITHIN* THE TOLERANCE LIMITS LISTED BELOW

BASIC DIM	DECIMAL 2 PLC	DECIMAL 3 PLC	FRACTIONS
UNDER 6"	± 0.02	± 0.010	± 1/32
6" TO 24"	± 0.03	± 0.020	± 1/16
ANGELS ± 1/2°			

PIN TYPE BEARING STRENGTH SPECIMEN

Figure 2. Single-hole pin-type bearing strength specimen configuration.

Test Techniques and Data Presentation

All tests were performed in accordance with ASTM Standard E-238 entitled "Pin-Type Bearing Test of Metallic Materials" except for the following. Since beryllium is a toxic material, special precautions were taken to prevent the escape of hazardous contamination from the specimen fracture. No additional work (machining, sanding, etc.) was done on the specimen hole because the specimens had been etched. Several different size pins were machined to compensate for the tolerances in the specimen hole. The pins were machined from 4340 steel with a hardness of HRC 60, and were centerless ground to size and polished to an 8 microinch finish. Specimens, pins, and fixtures were cleaned with MEK before

final assembly to ensure that there was no grease or contamination on the bearing surfaces. An MTS Model 623.028-20 clip gage, used to measure bearing strain, was attached to the specimen through an adaptor as shown in Figure 3. Tests were run under clip gage control so bearing strain rates were constant during the test. In this study specimens were tested at strain rates of 10^{-4}, 10^{-2}, and 1.0 per second. The load, displacement, bearing strain (clip gage), and time were recorded on the data acquisition and control system. All tests were conducted at room temperature and a relative humidity of approximately 70%.

A few technical terms, as defined in ASTM Standard E-238, are listed here for clarification and uniformity in our data analysis and presentation.

(1) Bearing Area - the product of the pin diameter and the specimen thickness.

(2) Bearing Stress - the force per unit of bearing area.

(3) Bearing Strain - the ratio of the bearing deformation of the bearing hole, in the direction of the applied force, to the pin diameter.

(4) Bearing Yield Stress - the bearing stress at which a material exhibits a specified limiting deviation from the proportionality of the bearing stress to the bearing strain.

(5) Bearing Strength - the maximum bearing stress which a material is capable of sustaining.

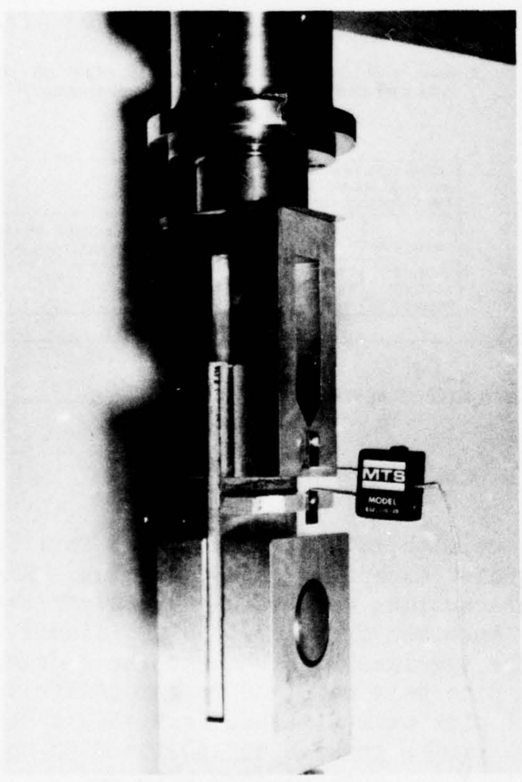

Figure 3. Grip and measuring arrangement for the single-hole bearing strength specimen.

(6) Edge Distance - the distance from the edge of a bearing specimen to the center of the hole in the direction of the applied force.

(7) Edge Distance Ratio - the ratio of the edge distance to the pin diameter.

Experimental Results and Discussions

Experimental results for the ASTM Standard pin-type bearing specimen of CIP/HIP-1 beryllium are summarized in Table 1. A typical bearing stress-strain curve obtained in this study is shown in Figure 4 which also shows the determination of the bearing yield stress according to the ASTM Standard. It is noticed that the bearing behaves elastically for bearing stress less than 20 ksi (137.9 MPa), beyond that the nonlinearity is observed.

Table 1. PIN-TYPE BEARING TEST RESULTS

Dir.	Spec. No.	T (in.)	Pin D (in.)	E Dist. (in.)	E/D Ratio	$\dot{\varepsilon}$ (sec^{-1})	2% Bearing Yield (ksi)	Bearing Strength (ksi)	% ε Max.	Net-Section Tensile Rupture Stress (ksi)
Specimen Group 1										
Z	BF 11	0.25	0.5	0.75	1.5	0.0001	-	98.6	3.70	19.7
Z	13					0.0001	89.0	99.0	4.20	19.8
Z	14					0.0001	88.5	98.1	4.17	19.6
Z	15					0.0001	88.3	98.7	4.17	19.7
Z	20					0.0001	86.5	100.3	4.80	20.1
Z	25					0.0001	90.6	100.2	4.84	20.0
Z	21					0.01	91.0	100.4	4.10	20.1
Z	22					0.01	90.0	99.2	4.27	19.8
Z	23					0.01	89.5	100.4	4.35	20.1
Z	24					0.01	91.0	100.4	3.94	20.1
Z	16					1.0	94.0	100.2	3.94	20.0
Z	17					1.0	92.5	100.3	4.30	20.1
Z	18					1.0	93.0	100.6	4.18	20.1
Z	19					1.0	92.5	97.3	3.62	19.5
X	BH 1					1.0	-	84.3	2.41	16.9
X	2					1.0	92.0	105.6	4.53	21.1
X	3					1.0	-	78.5	2.08	15.7
X	4					1.0	94.0	101.9	4.17	20.4
X	5					1.0	94.0	101.5	4.22	20.3
Specimen Group 2										
Z	BG 26	0.25	0.5	1.00	2.0	0.0001	97.0	114.1	5.08	22.8
Z	27					0.0001	102.5	120.5	5.02	24.1
Z	28					0.0001	102.0	118.8	5.00	23.7
Z	29					1.0	112.0	119.7	4.40	23.9
Z	30					1.0	106.5	122.0	4.38	24.4
Specimen Group 3										
Z	BJ 1	0.30	0.625	0.938	1.5	0.0001	89.0	95.8	4.00	25.2
Z	2					0.0001	88.5	97.1	4.17	25.6
Z	3					1.0	93.5	95.2	3.70	25.1
Z	4					1.0	94.0	94.0	3.10	24.7
Z	5					1.0	92.0	98.4	3.63	25.9
Specimen Group 4										
Z	BK 6	0.30	0.625	1.25	2.0	0.0001	103.5	118.1	4.47	31.08
Z	7					0.0001	109.0	111.7	4.16	29.4
Z	8					1.0	107.0	116.9	3.77	30.8
Z	9					1.0	111.5	120.2	4.14	31.6
Z	10					1.0	111.0	117.7	3.91	31.0

Note: 1 in. = 2.54 cm
1 ksi = 6.89 MPa

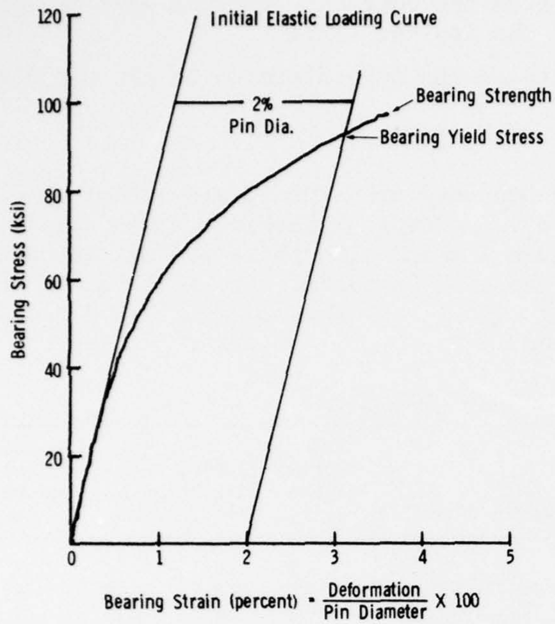

Figure 4. Typical bearing stress versus bearing strain curve for CIP/HIP-1 beryllium at a strain rate of 1 sec^{-1}.

Table 1 shows that for specimens of Group 1 which gives E/D=1.5, there is no strain rate effect on the bearing strength but there is a slight increase in bearing yield strength with increase of strain rates from 10^{-4} to 1.0 per second.

Specimens of Group 2, which gives E/D=2.0, were tested at two strain rates: 10^{-4} and 1.0 per second. Results show no strain rate effect on bearing yield stress and bearing strength, but a slight decrease in the maximum strain. However, by comparison of results from Groups 1 and 2, we notice that by increasing the edge distance or the ratio of E/D from 1.5 to 2.0, the bearing yield stress, bearing strength, and the maximum strain are increased.

Specimens of Groups 3 and 4 were tested at strain rates of 10^{-4} and 1.0 per second. From Table 1, we notice that results from Group 3 agree very well with those from Group 1, and Group 4 agrees well with Group 2. In other words, the bearing yield stress, bearing strength, and maximum strain will have the same value if specimens have the same ratio of edge distance to hole diameter (E/D) and maintain the ratio of hole diameter to plate thickness (D/T) between 2 to 4. However, the larger E/D ratio (E/D=2.0) gives a larger value of bearing yield stress, bearing strength, and maximum strain.

As mentioned in Section II, five Group 1 type specimens were taken from the hollow cylinder in such a way that the loading direction of the bearing test specimen was along the circumferential direction of the hollow cylinder. These specimens were tested at a strain rate of 1.0 per second and results were compared with other Group 1 type specimens tested at the same condition. There appears to be no directional effect on the bearing stress-strain responses. This conclusion agrees with the findings in References 1 and 2 which show that the CIP/HIP-1 fabrication process provides an isotropic structure.

Figure 5 shows the dimensions and typical patterns of fracture for the pin-type bearing test specimens. The fracture of both specimens initiated at the edge of the circular hole and about 90° from the direction of the load where the tensile stress is assumed to be a maximum. In general, there are three failure modes to be considered in the design of bolted or riveted joints transmitting loads through shear; namely, shear tear out of the plate, shear failure of the pin, and the tensile rupture of the plate. Their respective allowable stresses are usually specified in design codes. Since the failure pattern of the specimens tested appears to be tensile rupture of the plate, the tensile stress in the net section of the plate (load/(width minus hole diameter) × thickness) was calculated and listed in the last column of Table 1. It is noticed that the net section tensile rupture stress increases as the ratio of E/D or the thickness of the plate increases. This observation raises a question of whether the concept of allowable net section tensile stress for designing bolt joints is applicable in this study. A simple calculation can answer this question. From Reference 3 one can find the stress concentration factor K_{tnb} for a pinned or riveted joint with various geometries. Once the value of K_{tnb} is known, the maximum stress, σ_{max}, can be calculated by using the following equation

$$K_{tnb} = \left(\sigma_{max}/\sigma\right)\ (D/B)$$

where σ is the gross section stress, D is the hole diameter, and B is the distance between the neighboring holes which is the width of the specimen for the pin-type bearing test specimen. The values of σ_{max} for the four groups investigated are

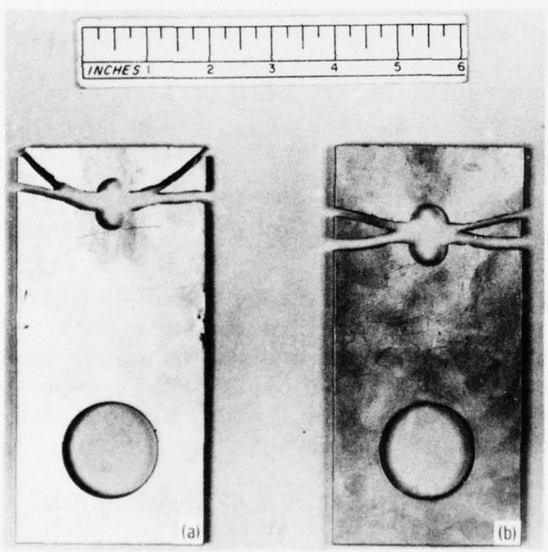

T, in. (cm) = 0.25 (0.635)	T, in. (cm) = 0.30 (0.762)
D, in. (cm) = 0.5 (1.27)	D, in. (cm) = 0625 (1.588)
E/D = 1.5	E/D = 2.0

Figure 5. Failure patterns of the single-hole pin-type specimen.

3. PETERSON, R. E. *Stress Concentration Factors.* John Wiley and Sons, New York, 1974, p. 215-216.

listed in Table 2. All four groups failed when the tensile stress reached a maximum value of approximately 115 ksi (792 MPa), even though their bearing strength and net section tensile rupture stress appear different from each other. This indicates that the allowable net section tensile stress may not be a workable criterion in designing bolted joints of a CIP/HIP-1 beryllium structure.

Table 2. CALCULATED MAXIMUM STRESS VALUES AND STRESS CONCENTRATION FACTORS FOR PINNED JOINT SPECIMENS

	D/B	$\frac{E-D/2}{D}$	K_{tnb}	Average Gross Stress (ksi)	σ_{max} (ksi)	σ_{max}/σ
Group 1	0.167	1.0	1.15	16.67	115.02	6.9
Group 2	0.167	1.5	1.0	19.81	118.9	6.0
Group 3	0.208	1.0	1.2	20.03	115.37	5.76
Group 4	0.208	1.5	1.0	24.37	116.95	4.8

Note: 1 ksi = 6.89 MPa

Another comment that should be made here is that the maximum tensile stress of 115 ksi (792 MPa), calculated from the stress concentration factor, is much higher than σ_{ult}=65∿70 ksi (448∿482 MPa) obtained from testing tension specimens (see Reference 1). This deficiency is probably due to the basic assumption of elastic behavior of materials in the derivation of stress concentration factor K_{tnb}, which was used in estimating the value of σ_{max}.

It is recognized that in the derivation of K_{tnb}, the effect of interaction between neighboring holes is included. However, this will not affect the conclusions drawn from this experimental study, because stress values calculated (see Table 2) are for the purpose of comparison only. The comparison is consistent in that all specimens have the same general configuration, i.e., a single pin hole.

IV. CIRCUMFERENTIAL SPLICE JOINT TESTS

In the previous section the basic data on a single-pin jointed specimen was discussed; however, in a real structure more than one bolt is required, and frequently it is necessary to use more than one row of bolts to connect the structural components together. The objective of this task is to investigate the effects of pitch (the distance between two holes) and various patterns of holes on the load-carrying capability of splice joints.

Specimen Configuration

The effects of pitch and hole patterns on the load-carrying capability of splice joints are investigated by testing three different types of splice joints. Figure 6 shows the detailed dimensions of all specimens, and Figure 7 shows a typical set of specimens for each type of splice joint, where a set consists of two main plates and one splice plate (cover plate). View a in these figures represents type 1, a single-bolted butt joint. The term single-bolted (or double-bolted, etc.) refers to the number of rows of bolts which transfer the total load

NOTES:

1. REMOVE ALL BURRS AND BREAK SHARP EDGES.
2. SURFACE FINISH TO BE 32 RMS.
3. ETCH ALL SURFACES TO FINISH DIMENSIONS, 0.004/0.005 PER SURFACE.
4. MARK APPLICABLE SPECIMEN IDENTIFICATION NUMBER IN 1/8" CHARACTERS WITH BLACK INK OR ELECTRO ETCH.
5. EACH SPECIMEN CONSIST OF TWO (A) AND ONE (B).
6. (A) = MAIN PLATE, (B) = SPLICE PLATE.

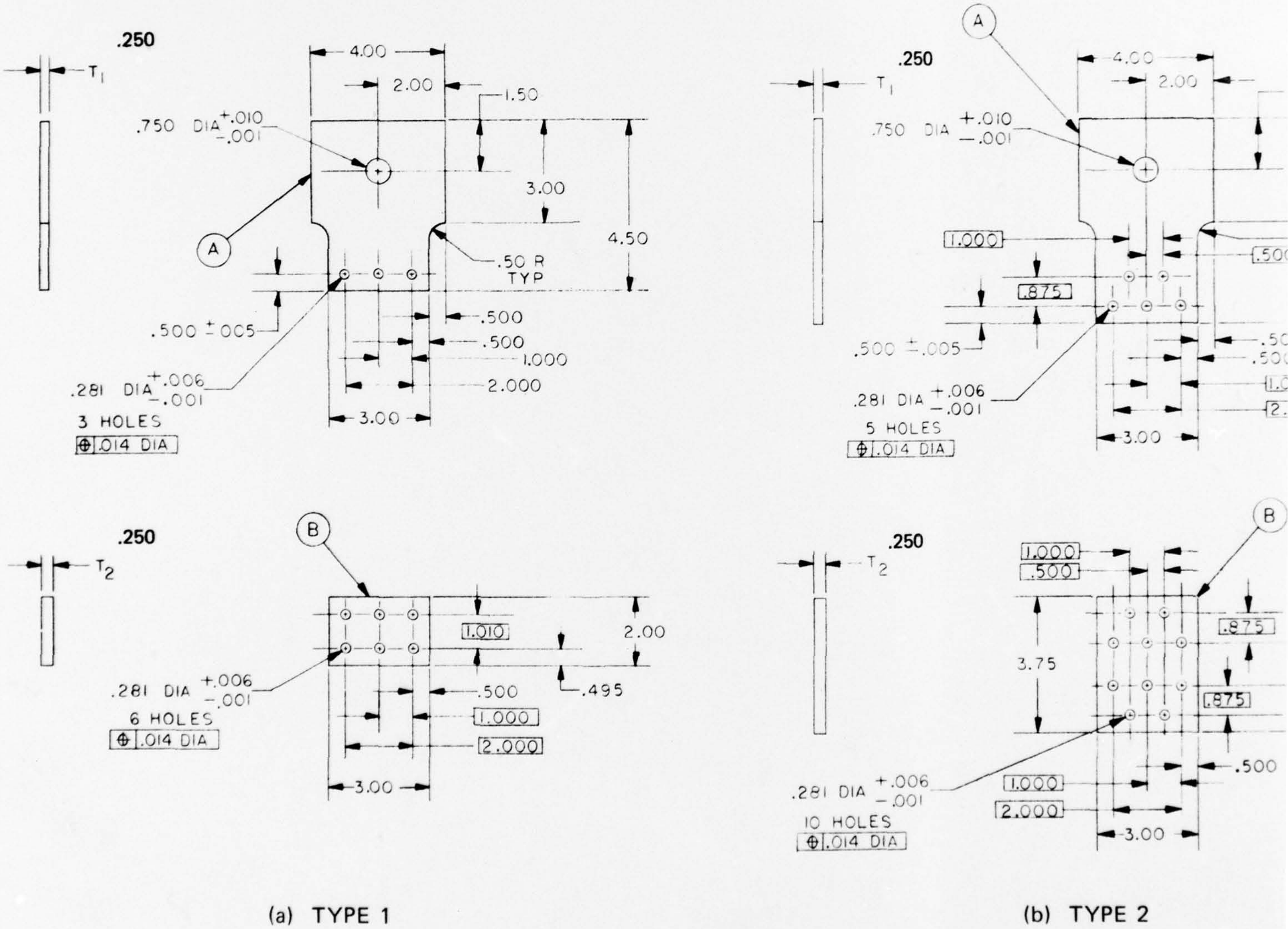

Figure 6. Joint-circumferential splice specimen configuration for b

UNLESS OTHERWISE SPECIFIED DIMENSIONS ARE IN INCHES AND ARE AFTER PLATING TOLERANCES ON:						
FRACTIONS	DECIMALS X	DECIMALS XX	DECIMALS XXX	ANGELS		SPECIMEN DEFINITION JOINT - CIRCUMFERENTIAL SPLICE
± ___	± ___	± 0.03	± 0.010	± 30′		

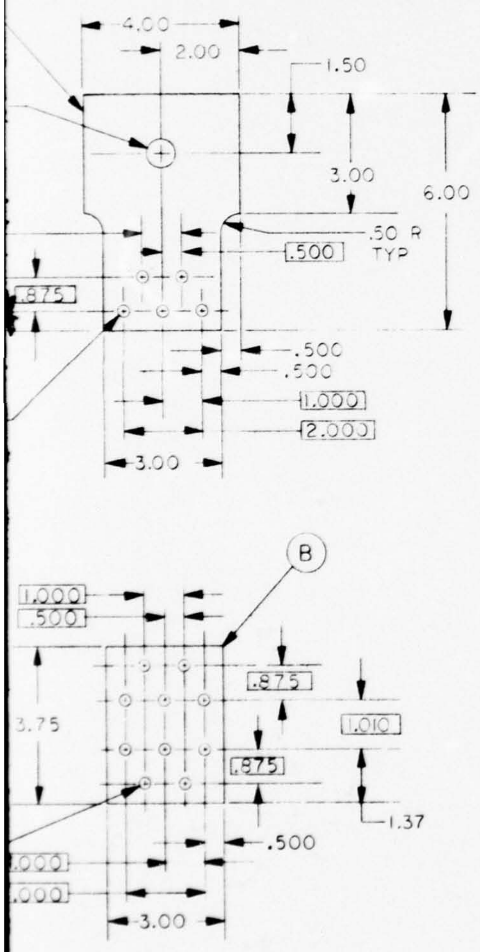

(b) TYPE 2

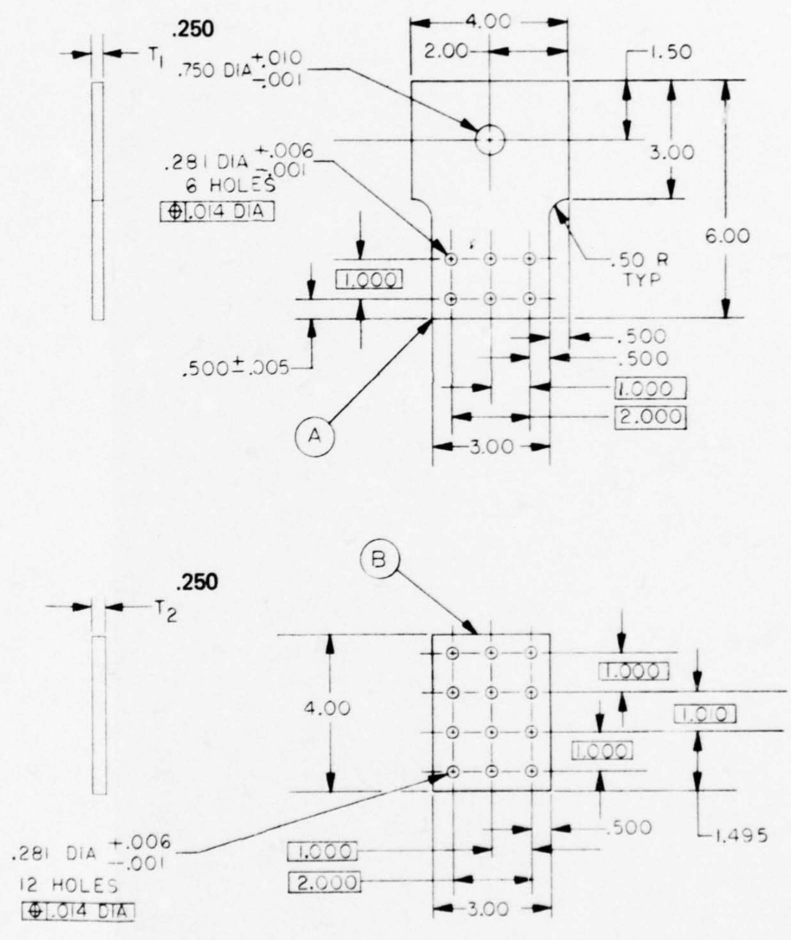

(c) TYPE 3

ice specimen configuration for bearing strength tests.

THIS PAGE IS BEST QUALITY PRACTICABLE
FROM COPY FURNISHED TO DDC

2

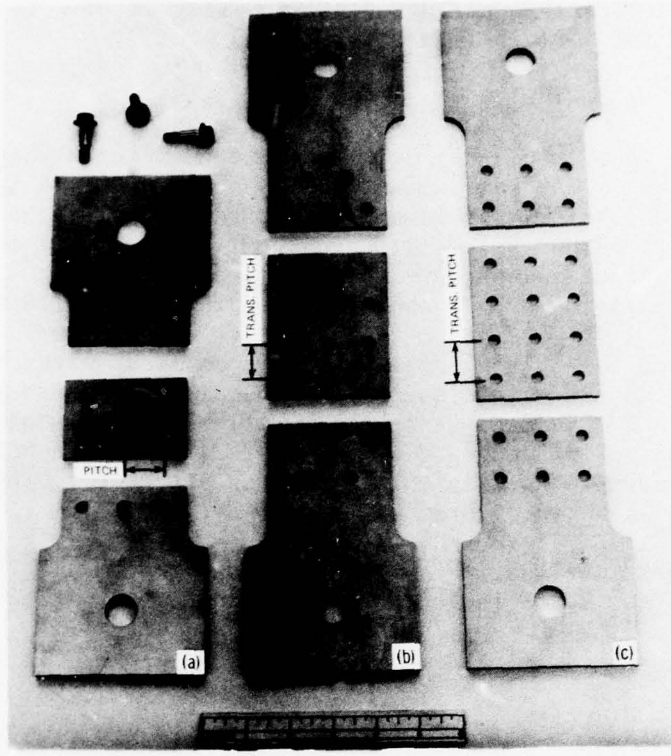

Figure 7. Joint-circumferential splice specimens and shoulder bolts.

from one element to another, for example, from main plate to cover plate or from cover plate to main plate. View b represents type 2, a double-bolted butt joint with a diamond pattern of holes, while view c represents type 3, also a double-bolted butt joint but with a square pattern of holes. At one end of each main plate there is a 0.750-inch-diameter (1.91 cm) hole so that a pin type of load train can be used to test the specimen, and the other end has one of the three different types of bolted joints. All bolt holes have a diameter D of 0.281 inch (0.71 cm) and a pitch of 1.0 inch (2.54 cm) (Figure 7). The transverse pitch is 0.875 inch (2.22 cm) for the diamond pattern (type 2), and 1.0 inch (2.54 cm) for the square pattern (type 3). With a width of 3 inches for the main plate, the single-bolted joint has 3 bolt holes, the diamond pattern joint has 5 bolt holes, and the double-bolted square pattern has 6 holes. The edge distance E for all specimens is 0.5 inch (1.27 cm) which gives the ratio of E/D=1.78, within the range of 1.5 and 2.0 specified by the ASTM Standard E-238.

Test Conditions

Every set of specimens consists of three pieces: two identical main plates and one splice plate. These three pieces were connected together by using either hardened pins or shoulder bolts and nuts as shown in Figure 7, and an assembled

set in the load train is shown in Figure 8. When shoulder bolts and nuts were used, the amount of torque required for a given size of bolt to tighten the nuts is calculated from the formula (see Reference 4)

$$PL = RDT$$

where PL is torque in inch-pounds; R is a torque coefficient depending on frictional conditions; D is the bolt diameter in inches; and T is tensile load in pounds. The shoulder bolts used have 1/4-20 thread, and if the maximum bolt stress is limited to 60,000 psi (414 MPa), the tensile load T equals 3000 pounds (13.34 kN). For ordinary steel nuts and bolts, driven dry in steel, R approximates 0.2. The corresponding torque is then equal to 150 lb-in. (16.95 N-m).

The response of the splice joint was shown as load versus the relative displacement between the two main plates. In order to be consistent with the measurement from the ASTM Standard test, the relative displacement must be measured at locations where the influence of the joint is minimum. A DCDT (Direct Current Differential Transformer) used in this study was attached to the top and bottom grip assemblies as shown in Figure 8.

One of the questions that may be raised by designers is: How important is it to achieve this torque level in the assembly procedure of structures. To answer

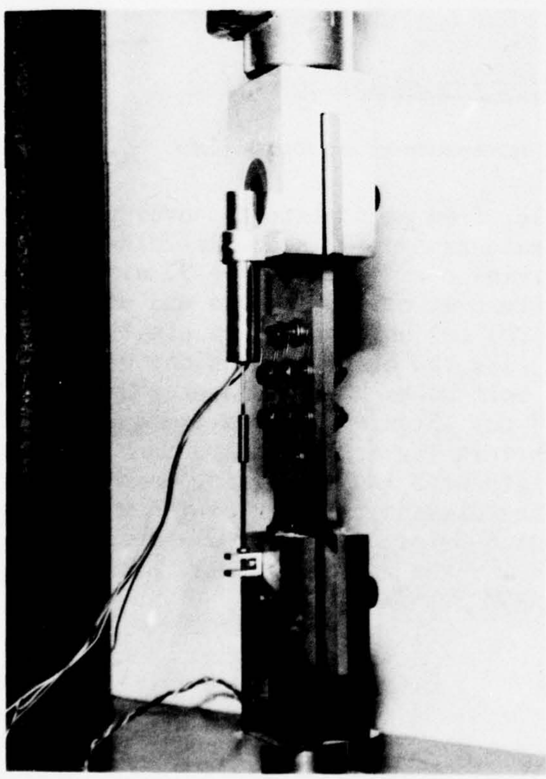

Figure 8. Grip and measuring arrangement for the joint-circumferential splice specimen.

4. CARMICHAEL, C. *KENT'S Mechanical Engineers Handbook.* Design and Production Volume, John Wiley and Sons, New York, 1950, p. 10-57.

this question, two extreme conditions were tested: one at no torque at all (i.e., the main plates are connected to the splice plate with pins only); and the other with the bolts torqued to the allowable value of 150 lb-in. (16.95 N-m). An interesting phenomenon was observed from testing bolted specimens, i.e., when a test specimen was assembled outside the test machine with fully torqued bolts and nuts, the load versus displacement curve exhibited a slippage of joints at a certain level of load. This is attributed to nonuniform clearances in the hole. When the load exceeded the frictional force between the main plate and splice plate, which is proportional to the tensile stress in the bolts (or torque), a slippage between the plates occurred. This phenomenon was eliminated by hand tightening the bolts outside the test machine, then the set of specimens was assembled in the load train and preloaded to 500 pounds (2.22 kN) before all bolts were tightened by a torque wrench to the allowable torque value of 150 lb-in. (16.95 N-m).

Results and Discussions

As mentioned earlier, three types of circumferential splice joints were tested in this study. Type 1 is a single-bolted butt joint; type 2 is a double-bolted butt joint with a diamond pattern of holes; and type 3 is a double-bolted butt joint with a square pattern of holes. There are five sets of specimens for each type of splice joint. Table 3 lists the fasteners (i.e., either pins or

Table 3. CIRCUMFERENTIAL SPLICE JOINT SPECIMENS OF CIP/HIP-1 BERYLLIUM

Spec. No.	No. Holes	Thick. (in.)	Max. Load (lb)	Max. Deflect (in.)	Fasteners	Torque (lb-in.) on Bolts	Preload Before Applied Torque (lb)
Type 1							
16 BU	3	0.254	12,980	0.092	Pins	0	0
17	3	.255	12,150	.016	Pins	0	0
18	3	.255	13,950	.110	Pins	0	0
19	3	.2525	13,800	.062	Bolts	150	500
20	3	.256	15,080	.071	Bolts	150	500
		Avg. Pinned	13,000	0.103			
		Bolted	14,400	.067			
Type 2							
21 BV	5	0.254	16,200	0.104	Pins	0	0
22	5	.255	18,380	.138	Pins	0	0
23	5	.255	18,880	.107	Bolts	150	0
24	5	.254	15,500	.068	Bolts	150	0
25	5	.255	16,250	.069	Bolts	150	500
		Avg. Pinned	17,300	0.121			
		Bolted	16,900	.081			
Type 3							
26 BW	6	0.254	18,690	0.110	Bolts	150	0
27	6	.255	18,180	.097	Bolts	150	0
28	6	.253	15,890	.097	Pins	0	0
29	6	.2555	18,130	.090	Bolts	150	500
30	6	.2550	14,320	.058	Bolts	150	500
		Avg. Pinned	15,900	0.097			
		Bolted	17,300	.089			

Note: 1 in. = 2.54 cm
1 ksi = 6.89 MPa
1 lb = 4.448 N
1 lb-in. = 0.1130 N-m

bolts) used for each set of specimens, and also shows the maximum load and deflection of each test. The load versus displacement curves for the three types of specimen configurations are shown in Figure 9.

For the type 1 specimens, Figure 9a shows that the bolted joint gives a slightly higher load at failure but less maximum deflection than the pinned joint. The bolted joint also provides a much higher stiffness than the pinned joint. This suggests that if splice joints were used to assemble structural components, the maximum allowable bolt torque should be used to provide the highest possible stiffness of the joints. The load versus displacement of specimen 19 BU shows a discontinuity of a load about 14,000 lb (62.3 kN); this is due to a crack developed from the side edge of the splice plate to the nearest hole before catastrophic failure of the specimen occurs. A loud cracking noise was heard during the test of specimen 19 BU when the crack developed.

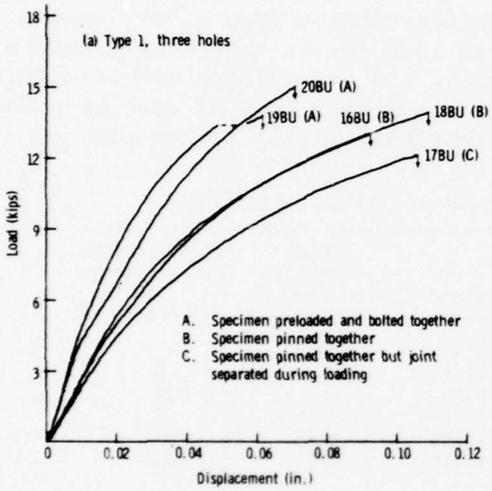

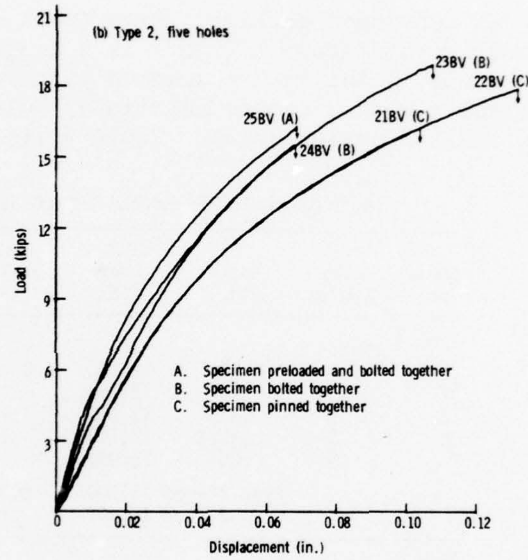

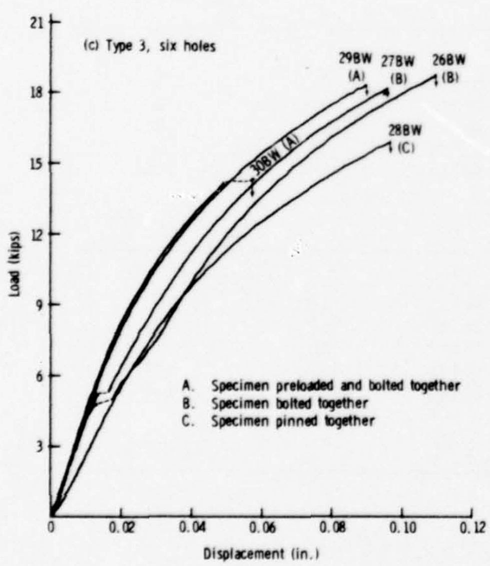

Figure 9. Load versus displacement curves for circumferential splice joint specimens of CIP/HIP-1 beryllium.

Figure 9b shows the load versus displacement curves of the type 2 specimens. There is a distinct difference in the response of bolted joint specimens assembled with and without preload. The bolted joint assembled without the preload shows a softening effect at the load level between 4000 and 5000 lb (17.8 and 22.2 kN), then it becomes stiffer again. This is attributed to the nonuniform clearance between the bolts and holes; when the load exceeds the frictional force between the main plates and splice plate, a slippage occurs until all bolts fully contact the inner surface of the holes.

An estimation can be made to show that the attribution is a reasonable assumption. As it was discussed earlier, the tensile force in the bolt was 3000 lb (13.3 kN) with a bolt torque of 150 lb-in. (16.95 N-m). Since type 2 specimens have five bolts the total normal force on the interface between the main plate and splice plate is 15,000 lb (66.7 kN). If the slippage occurs at 4000 to 5000 lb (17.8 to 22.2 kN), the coefficient of friction is between 0.267 and 0.333, which is an acceptable value for the etched surfaces of the tested specimens. Again, the pinned joint is not as stiff as the bolted joint, and it has more displacement at failure. However, there is no clear trend as far as the maximum load is concerned.

The load versus displacement curves for the type 3 specimens are shown in Figure 9c. The bolted joint specimens without the preload generated distinct cracking noises during the test at approximately 5000 lb (22.2 kN) load when sharp breaks in the curves were observed. Since type 3 specimens have six bolts, the normal force between the main plate and splice plate is 18,000 lb (80.1 kN). The slippage occurs at 5000 lb (22.2 kN) load which gives a coefficient of friction equal to 0.267. This agrees very well with the estimated frictional coefficient for type 2 specimens. The sharp breaks in the curve disappear when a preload of 500 lb (2.22 kN) was used during the assembly of the specimens. One of the five sets of specimens is pin jointed and it shows a lower maximum load at failure.

One of the drawbacks of testing splice joint specimens with one cover plate is that the axis of load is always eccentric with respect to the joint, and a bending moment is induced in the joint which is proportional to the axial load. Since the pinned joint has no lateral constrained force, it is expected that the undesirable bending moment is larger in the pinned joint than in the bolted joint. This is confirmed by the post mortem examination of ruptured specimens shown in Figure 10. The cover plate and main plate of the pinned joint are permanently separated due to the out-of-plane deformation of the cover plate, while the bolted joint shows practically no separation at all. If the effect of this bending moment is neglected in the stress analysis, one can again use the curves provided in Reference 3 to estimate the maximum stress since all specimens failed in the tensile rupture mode. The geometry parameters for specimens used in this study are larger than those in Reference 3; therefore the stress concentration factor K_{tnb} used to estimate maximum stresses is obtained through extrapolation, Table 4.

It is noticed that the values of σ_{max} at failure of the splice joint are less than those of the standard ASTM bearing test specimen; this reduction in strength is probably due to the interaction of neighboring holes. The test results in Table 4 also indicate that the maximum load of type 1 specimen is not equal to three times the maximum load of the standard bearing test specimen.

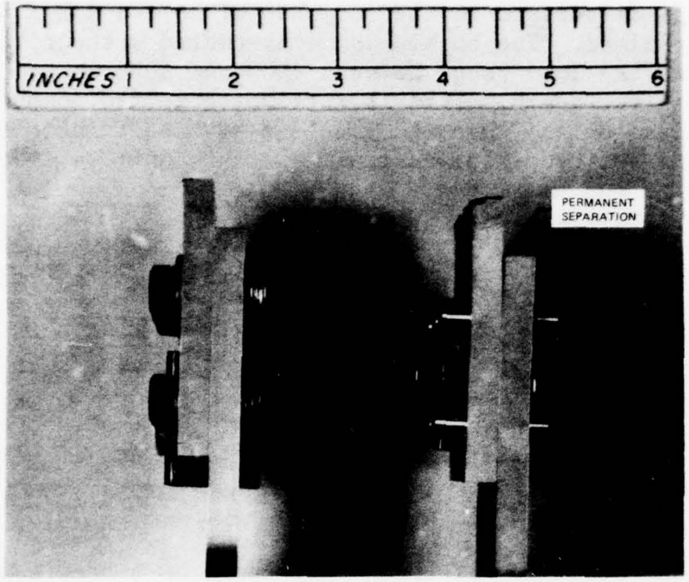

Figure 10. Side view comparing bending of the pinned- and bolted-type attachments for the joint-circumferential splice specimen.

Table 4. CALCULATED MAXIMUM STRESS VALUES AND STRESS CONCENTRATION FACTORS FOR SPLICE JOINT SPECIMENS

	D/B	$\frac{E-D/2}{D}$	K_{tnb}	Average Gross Stress (ksi)	σ_{max} (ksi)
Type 1	0.281	1.28	1.2	19.2	82.0
Type 2	0.281	1.28	1.2	22.5	96.1
Type 3	0.281	1.28	1.2	23.1	98.6

Note: 1 ksi = 6.89 MPa

The maximum loads at failure for type 2 and 3 specimens are practically the same; this suggests that the hole pattern and the transverse pitch have no effect on the load-carrying capability of the tested specimens. However, the maximum load for type 1 specimens is less than that for types 2 and 3; the reason for this is not clear from the strength of materials point of view, and further studies are required.

Typical failure patterns for each type of specimen are shown in Figure 11. Figure 11a (left) shows a failure occurred in the main plate which was pin jointed to the cover plate. This was the only specimen that failed in such a manner. The remaining type 1 specimens failed across the holes in the splice plate as shown in Figure 11a (right). Every type 2 and 3 specimen failed across the holes in the cover plate, except one specimen of each type failed in the gross section area as

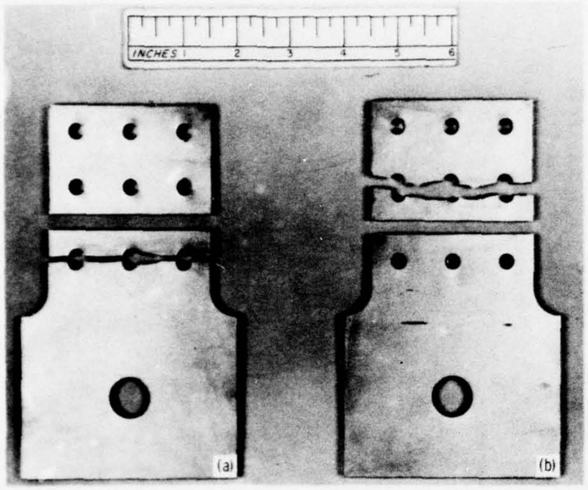

a. Three-hole joint

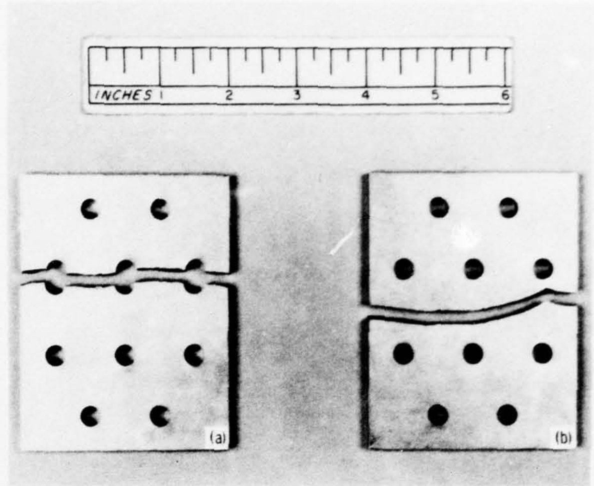

b. Five-hole joint

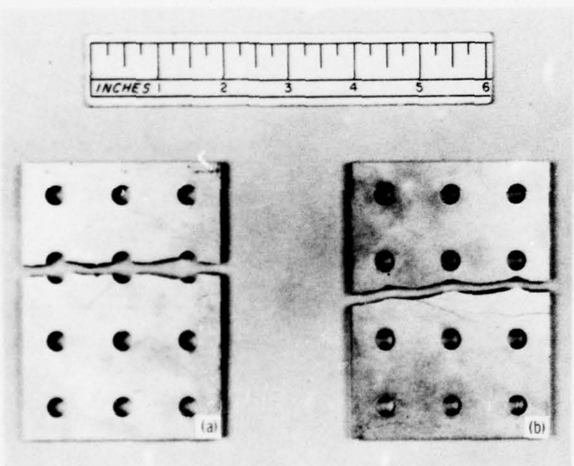

c. Six-hole joint

Figure 11. Failure patterns of the circumferential splice specimens.

shown on the right in Figures 11b and 11c. Both specimens which failed in the gross section area were bolted to the splice plate without the preload. This indicates that there were defects in the splice plates of these two specimens which caused a more severe stress concentration than the bolt holes.

We have found that for the specimen configurations and material used in this study the maximum stress, instead of the failure load and net cross section stress, should be used as a design criterion. For the double-bolted joint, the hole pattern and transverse pitch have no effect on the load-carrying capability of the joint. However, the correlation between results from the single-bolted joint and those from the double-bolted joint require further study.

APPENDIX. AUTOMATED MATERIALS CHARACTERIZATION SYSTEM

All bearing tests were performed on an automated materials characterization system, shown in Figure A-1, which consists of two principal components; namely, the medium strain rate machine and the data acquisition and control system. The medium strain rate machine (MSRM) is used to generate the axial loadings on the test samples. The data acquisition and control system generates command signals and records, stores, and analyzes data from the tests.

Medium Strain Rate Machine

The MSRM (Figure A-2) is a dual-mode testing machine. It has a capability of generating 140,000 pounds (623 kN) static load in tension or compression and has a piston displacement stroke of six inches. The load frame is designed for a stiffness of greated that 15×10^6 lb-in. (2.6×10^9 N-m) and has a total stretch of 0.005 inch (0.013 cm) at the maxium load. This machine also incorporates an automatic purging sequence which allows the interchange of operating modes for closed loop or open loop operation. A schematic of the controls for the MSRM is shown in Figure A-3.

In the open loop mode, which is gas operated, using either dry nitrogen or helium, strain rates of 1 to 50 sec^{-1} can be obtained by varying the charge pressure, orifice size, or length of piston travel (stroke).

Figure A-1. Automated materials characterization system.

PRECEDING PAGE NOT FILMED
BLANK

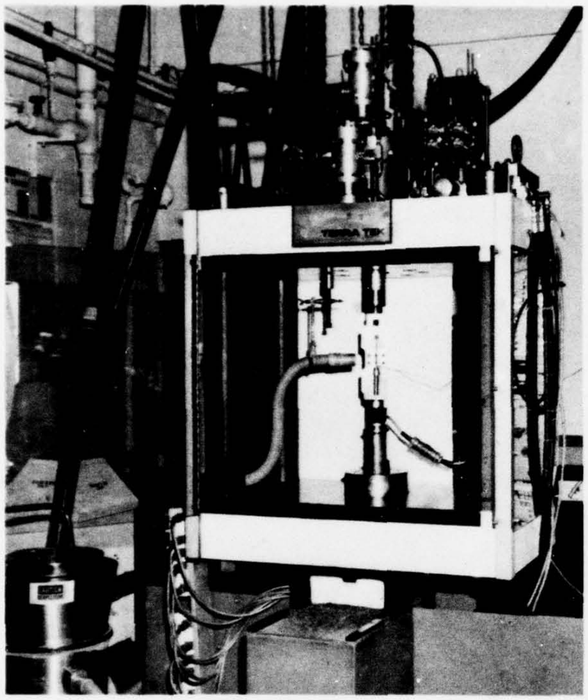

Figure A-2. Load frame and test set up using safety enclosure.

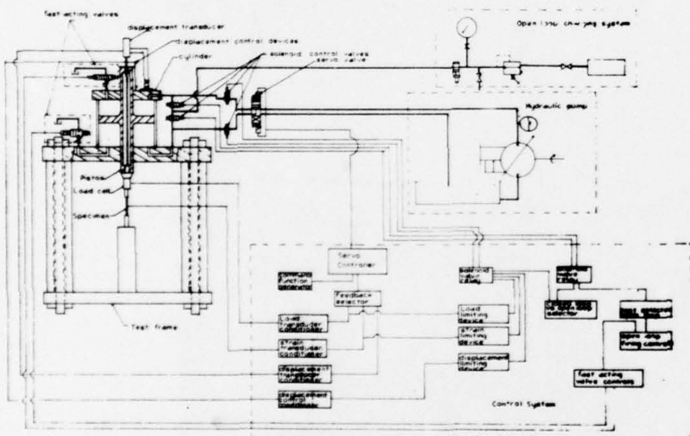

Figure A-3. Schematic of controls for the medium strain rate test machine.

The electrohydraulic (closed loop) mode of the test machine can control strain rates from 10^{-6} to 1 sec^{-1}. The closed loop control parameter of this machine permits the selection of four different feedback signals: load, displacement, strain, and optional. The optional control allows external transducers, such as clip gages or DCDT's, to be used for control and monitoring. With the proper command inputs, tests at constant rates of load, displacement, or strain can be performed. The operator may select one of many load transducers to achieve the best control of the desired testing range.

The MSRM is equipped with a servocontroller, four transducer conditioners, and various fail-safe devices. The transducer conditioners accept inputs from the transducers and amplify their voltage signals for feedback to the servocontroller and data acquisition system. The servocontroller compares the feedback signal with the command input signal (from the data acquisition and control system) and generates an error signal. This error signal drives a 15-gal/min electrohydraulic servovalve, which regulates the flow of oil from the hydraulic power supply to the machine actuator. The system is also incorporated with fail-safe circuits and limiting switches which can be set to display a warning light or abort the test.

Data Acquisition and Control System

The data acquisition and control system, Figure A-4, is a Digital Equipment Corporation PDP-12/40 computer which consists of a central processor, 4K words of basic memory, 12K words of extended memory, real-time clock, relay register, 1.6 million word removable disk pack, two magnetic tape drives, teletype, line printer, display screen, multiplexed analog-to-digital converter (16 channels), and three digital-to-analog converters. The system interface includes active filters and scaling amplifiers.

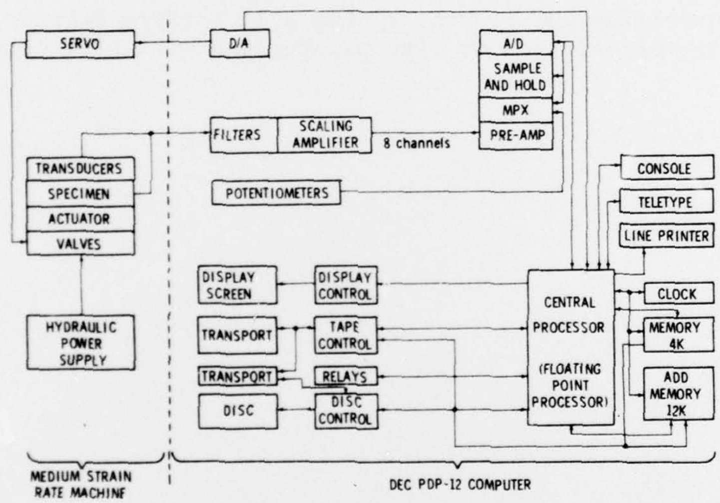

Figure A-4. Schematic for automated materials characterization system.

The digital computer uses its memory to hold the operating system, to store programs during execution, and for temporary storage of data. Command signals generated by the central processor are sent to the digital-to-analog (D/A) converters at predetermined intervals, by the real-time clock. The D/A converter changes the binary number (12 BITS) (which is the internal information base of the computer) to an analog voltage (±10 VDC), which is within the acceptable range of the servocontroller. The specimen load, displacement, strain, etc., are continuously monitored by the computer (see attached program listing). These

analog signals are filtered to remove noise, and scaled to match the range to the analog-to-digital (A/D) converter (±1 VDC). The multiplexer selects one of the 16 analog channels for input into the system. The analog signal is switched through the multiplexer to the sample and hold unit, which maintains the instantaneous analog voltage, until the A/D completes its conversion to a binary number (10 BITS). The data are then stored in memory, with other data points already taken from the test, and displayed on the screen for observation. A permanent file, on magnetic tape or disk, is created for the data and labeled with the test number. The real-time clock determines sampling intervals and command intervals or can be used to set time for other internal and external events. The teletype is an input-output (I/O) device used to transfer programs and parameters in and out of the system. Large outputs are printed on the high-speed line printer. The magnetic tapes and disk provide fast access to mass storage for programs and data. The relay register is used for additional control of the tests and external equipment.

When the MSRM is in the open loop mode, the computer uses a relay to initiate the test. The system samples load, displacement, strain, and time at the maximum rate permitted by the A/D converter. The data is temporarily stored in memory, and after completion of the test, the data is transferred to magnetic tape for permanent storage and for future data reduction.

The data acquisition and control system will perform data reduction and output the results on the teletype or line printer and will plot curves on an x-y recorder.

```
C     PROGRAM CLOSE -   CLOSE LOOP PROGRAM TAKING 256 DATA POINTS
C
C     1 TO 4 CHANNELS 1SEC TO 10 SEC 256 DA'S
C
C       NO DATA ANALYSIS
C
C
      DIMENSION A(256),B(256),C(256),D(256),PLTBUF(200),DATBUF(50)
      COMMON/D/A,B,C,D,PLTBUF,DATBUF
C
C       CREATE DATA FILE
C
      DEFINE FILE 1(4,256,U,L)
C
C       ZERO D/A
C
      CALL DTOA(1,0.0)
      N=1HN
      WRITE(4,2004)
 2004 FORMAT(' CLOSE - NO DATA ANALYSIS ',//)
C
C       NUMBER OF INPUT CHANNELS
C
   11 WRITE(4,1015)
      READ(4,5001) NUMCH
      IF(NUMCH.GT.4) GO TO 11
C
C       TOTAL TEST TIME (SEC)
C
   10 WRITE(4,1013)
      READ(4,5000) TIME
      IF(TIME.LT.1) GO TO 10
C
C       TENSION OR COMPRESSION ?
C
      WRITE(4,1010)
      READ(4,4001)TEST
 1068 WRITE(4,1069)
 1069 FORMAT(' TYPE RETURN TO GO',$)
      READ(4,4001) GO
 1010 FORMAT(' TEST TYPE : TEN OR COM:T OR C  -  ',$,1A4)
 1013 FORMAT(' TOTAL TEST TIME IN SECONDS = ',F10.2)
 1015 FORMAT(' # OF CHANNELS = ',I1)
 2000 FORMAT(1H1)
 2005 FORMAT(' SAVING DATA ON UNIT 1 ',1A1)
 4001 FORMAT(1A1)
 5000 FORMAT(I10)
 5001 FORMAT(I1)
  900 T=1HT
      CC=1HC
      Y=1HY
      NPTS=256
      IF(TEST.EQ.T) DA=-1.0
      IF(TEST.EQ.CC) DA=0.0
```

```
      CALL DTOA(1,DA)
C
C      SET UP FOR SCOPE DISPLAY
C
      CALL CLRPLT(200,PLTBUF)
      NDA=2048
      INCDA=-1
      IF(TEST.EQ.T) INCDA=-INCDA
      NCPTS=NPTS
      KK=(TIME/20.)+1
      CR=(KK*2048)/TIME
      NDAAD=2048/NPTS
      NTPTS=NUMCH*(KK*2048.)
      IF(TIME .LT. 9.99) NTPTS=NUMCH*NPTS
C
C      DATA ACQUISITION SUBROUTINE
C
      CALL REALTM(DATBUF,50,8,NUMCH,NTPTS)
      IF(TIME-9.99) 200,200,300
C
C      SHORT TEST 1-10 SECONDS
C
  200 CR=256/TIME
      INCDA=8
      IF(TEST .EQ. CC) INCDA=-INCDA
C
C      START INTERNAL CLOCK
C
      CALL CLOCK(0,CR)
      DO 201 I=1,256
      DA=DA+INCDA
      CALL DTOA(1,DA)
      A(I)=ADB(X)
      IF(NUMCH.EQ.1) GO TO 201
      B(I)=ADB(X)
      IF(NUMCH.EQ.2) GO TO 201
      C(I)=ADB(X)
      IF(NUMCH .EQ. 3) GO TO 201
      D(I)=ADB(X)
  201 CONTINUE
C
C      END OF FAST TEST
C
      GO TO 450
  300 CONTINUE
      DO 309 L=1,256
  309 CALL PLOT(1,0.,0.)
      CALL CLOCK(0,CR)
C
C      START OF SLOW TEST
C
      DO 301 I=1,NPTS
      CALL SSW(0,SW0)
      IF(SW0.EQ.1) GO TO 450
      DO 302 J=1,NDAAD
```

```
      DO 307 K=1,KK
      IF(K.NE.KK) GO TO 317
      IF(CONT.EQ.Y) GO TO 317
  315 DA=DA+INCDA
  316 CALL DTOA(1,DA)
  317 A(I)=ADB(X)
      IF(NUMCH.EQ.1) GO TO 307
      B(I)=ADB(X)
      IF(NUMCH.EQ.2) GO TO 307
      C(I)=ADB(X)
      IF(NUMCH.EQ.3) GO TO 307
      D(I)=ADB(X)
 307  CONTINUE
 302  CONTINUE
C
C       DISPLAY DATA WHILE TEST IN PROGRESS
C
  301 CALL PLOTR(1,C(I)*1.3/511.,A(I)/511.,I)
 450  CALL PLT4
C
C       STORES DATA IN FILE
C
 470  WRITE(4,2005)
      L=1
      WRITE(1'L) A
      L=2
      WRITE(1'L) B
      L=3
      WRITE(1'L) C
      L=4
      WRITE(1'L) D
      STOP
      END
```

```
C      PROGRAM BEAR
C
C     PIN BEARING STRENGTH
C
C

      DIMENSION A(256),B(256),C(256),D(256),PLTBUF(200),DATBUF(50)
      COMMON/Q/A,B,C,D,DATBUF,PLTBUF
      COMMON/QQ/ACAL,BCAL,CCAL,DCAL,T1
C
C       DEFINES DATA FILE
C
      DEFINE FILE 1(4,256,U,L)
      N=1HN
      WRITE(4,2004)
 2004 FORMAT(' BEAR - ANALYSIS OF PIN BEARING STRENGTH TEST ',//)
C
C       READ TEST NUMBER
C
```

```
      WRITE(4,1000)
      READ(4,4024)TNUM1,TNUM2
C
C      READ DATE
C
      CALL DATE(J1,J2,J3)
C
C      READ LOAD CALIBRATION
C
      WRITE(4,1002)
      READ(4,5000)XLCAL
C
C      READ SPECIMEN THICKNESS
C
      WRITE(4,2002)
      READ(4,5000)TH
C
C      READ TOTAL TEST TIME
C
      WRITE(4,1013)
      READ(4,5000) TIME
C
C      READ 3 DISPLACEMENTS
C
      WRITE(4,1204)
      READ(4,5000) D1
      WRITE(4,1004)
      READ(4,5000) D2
      WRITE(4,1007)
      READ(4,5000) D3
C
C      READ NUMBER OF PINS
C
      WRITE(4,1005)
      READ(4,5001) NN
C
C      READ PIN DIAMETER
C
      WRITE(4,1006)
      READ(4,5000) PDIA
      BA=PDIA*TH*NN
   11 CONTINUE
 1000 FORMAT(' TEST NUMBER = ',2A4)
 1001 FORMAT(' DATE IS =  ',I3,I3,I5,//)
 1002 FORMAT(' LOAD CAL. = ',F10.1)
 1004 FORMAT(' CH #12 DISP CAL = ',F10.4)
 1005 FORMAT(' NO. OF PINS ',I5)
 1006 FORMAT(' PIN DIAMETER ',F10.4)
 1007 FORMAT(' CH #13 DISP CAL = ',F10.4)
 1013 FORMAT(' TOTAL TEST TIME IN SECONDS = ',F10.2)
 2002 FORMAT(' SPEC THICK = ',F10.4)
 2000 FORMAT(1H1)
 1204 FORMAT(' CH #11 DISP CAL = ',F10.4)
 1207 FORMAT(' CHANNEL #11 STRAIN CALIBRATION = ',F10.4,' PERCENT',
 4001 FORMAT(1A1)
 4024 FORMAT(2A4)
```

```
      5000 FORMAT(I10)
      5001 FORMAT(I1)
      5002 FORMAT(I2)
      5003 FORMAT(I3)
      6001 FORMAT(' CHANNEL #12 STRAIN CALIBRATION = ',F10.4,' PERCENT',
      6002 FORMAT(' CHANNEL #13 STRAIN CALIBRATION = ',F10.4,' PERCENT',
      6003 FORMAT(' STRESS     CH# 11    CH# 12    CH# 13    TIME     STRAIN
          1')
      6004 FORMAT('   KSI      STRAIN    STRAIN    STRAIN    SEC      RATE
          1',//)
      6006 FORMAT(F8.2,F9.3,F9.3,F9.3,F8.2)
      6007 FORMAT(F8.2,F9.3,F9.3,F9.3,F8.2,F10.5)
      6010 FORMAT(' STRESS CAL = ',F10.3,' KSI ')
           Y=1HY
C
C        READ RAW DATA FROM FILE
C
       465 L=1
           READ(1'L) A
           L=2
           READ(1'L) B
           L=3
           READ(1'L) C
           L=4
           READ(1'L) D
C
C*       CROSS PLOTTING SUBROUTINE
C
           CALL PLT4
C
C        OUTPUT TEST PARAMETERS LO LINE PRINTER
C
       480 WRITE(3,1000)TNUM1,TNUM2
           WRITE(3,1001)J1,J2,J3
           STRESS=XLCAL/BA/1000.
           WRITE(3,6010) STRESS
           WRITE(3,2002)TH
           WRITE(3,1005) NN
           WRITE(3,1006) PDIA
           WRITE(3,1204) D1
           STC11=D1/(PDIA)*100.
           WRITE(3,1207) STC11
           WRITE(3,1004)D2
           STC12=D2/(PDIA)*100.
           WRITE(3,6001)STC12
           WRITE(3,1007)D3
           STC13=D3/(PDIA)*100.
           WRITE(3,6002)STC13
           WRITE(3,1013) TIME
           WRITE(3,2006)
           WRITE(3,1000)TNUM1,TNUM2
           WRITE(3,1001)J1,J2,J3
C
C        OUTPUT BEARING STRESSES,STRAINS,TIMES,&SRTAIN RATES
C
```

```
      WRITE(3,1402)
 1402 FORMAT(' BEARING STRESSES & STRAINS ')
      WRITE(3,6003)
      WRITE(3,6004)
      J=52
      ACAL=STRESS/511.
      BCAL=STC11/511.
      CCAL=STC12/511.
      DCAL=STC13/511.
      TI=TIME/256
      DO 510 I=1,256
      CALL SSW(0,ISNS0)
      IF(ISNS0.EQ.1) GO TO 600
      IF(I.NE.J) GO TO 511
      WRITE(3,2000)
      WRITE(3,1000)TNUM1,TNUM2
      WRITE(3,1001)J1,J2,J3
      WRITE(3,6003)
      WRITE(3,6004)
      J=J+52
  511 STR=A(I)*ACAL
      EB=B(I)*BCAL
      EC=C(I)*CCAL
      ED=D(I)*DCAL
      TM=TI*I
      IF(I.GT.15) GO TO 509
      WRITE(3,6006)STR,EB,EC,ED,TM
      GO TO 510
  509 SR=(C(I)-C(I-15))*CCAL/(TI*15)/100.
      WRITE(3,6007)STR,EB,EC,ED,TM,SR
  510 CONTINUE
      WRITE(3,2000)
      WRITE(3,2000)
  600 CONTINUE
C
C       PLOT STRESS-STRAIN CURVE ON X-Y RECORDER ?
C
      WRITE(4,1025)
 1025 FORMAT(' DO YOU WANT A STRESS VS STRAIN PLOT - ')
      READ(4,4001)PL
      IF(PL.NE.Y) CALL EXIT
      CALL XYREC4
      STOP
      END
```

DISTRIBUTION LIST

No. of Copies	To
	Office of the Under Secretary of Defense for Research and Engineering, The Pentagon, Washington, D.C. 20301
1	ATTN: Mr. J. Persh, Staff Specialist for Materials and Structures (Room 3D1089)
12	Commander, Defense Documentation Center, Cameron Station, Bldg. 5, 5010 Duke Street, Alexandria, Virginia 22314
	Deputy Chief of Staff, Research, Development, and Acquisition, Washington, D.C. 20310
1	ATTN: DAMA-CSS-D/Dr. J. I. Bryant (Room 3D424)
	Commander, U. S. Army Materiel Development and Readiness Command, 5001 Eisenhower Avenue, Alexandria, Virginia 22333
1	ATTN: DRCLDC, Mr. R. J. Zentner
	Director, Ballistic Missile Defense Systems Command, P. O. Box 1500, Huntsville, Alabama 35807
1	ATTN: BMDSC-TEN, Mr. N. J. Hurst
1	BMDSC-H
1	BMDSC-T
1	BMDSC-AOLIB
	Ballistic Missile Defense Program Office, DARCOM Bldg, Seventh Floor, 5001 Eisenhower Avenue, Alexandria, Virginia 22333
1	ATTN: DACS-BMT
	Director, Ballistic Missile Defense Advanced Technology Center, P. O. Box 1500, Huntsville, Alabama 35807
1	ATTN: ATC-M, Mr. M. Whitfield
1	ATC-M, Dr. D. Harmon
1	ATC-M, Mr. J. Papadopoulos
	Director, Defense Nuclear Agency, Washington, D.C. 20305
1	ATTN: SPAS, Mr. J. F. Moulton, Jr.
1	SPAS, Mr. D. Kohler
	Commander, U. S. Army Ballistic Research Laboratories, Aberdeen Proving Ground, Maryland 21005
1	ATTN: DRDAR-BLT, Dr. N. J. Huffington, Jr.
1	DRDAR-BLT, Dr. T. W. Wright
1	DRDAR-BLT, Dr. G. L. Moss
	Commander, Harry Diamond Laboratories, 2800 Powder Mill Road, Adelphi, Maryland 20783
1	ATTN: DELHD-NP, Dr. F. Wimenitz

No. of Copies	To
	Commander, U. S. Army Combat Development Command, Institute of Nuclear Studies, Fort Bliss, Texas 79916
1	ATTN: Technical Library
	Commander, Air Force Materials Laboratory, Air Force Systems Command, Wright-Patterson Air Force Base, Ohio 45433
1	ATTN: LNE/Dr. W. Kessler
1	LNC/Dr. D. Schmidt
	Space and Missile Systems Organization, P. O. Box 92960, World Way Postal Center, Los Angeles, California 90009
2	ATTN: RSSE/LTC J. McCormack
	Commander, Naval Ordnance Systems Command, Washington, D.C. 20360
1	ATTN: ORD-03331, Mr. M. Kinna
	Commander, Naval Surface Weapons Center, Silver Springs, Maryland 20910
1	ATTN: Dr. C. Lyons
1	Dr. W. Messick
	Naval Air Development Center, Warminster, Pennsylvania 18974
1	ATTN: G. L. London (Code 3023)
	Aerospace Corporation, P. O. Box 92957, Los Angeles, California 90009
1	ATTN: Dr. R. Cooper
1	Dr. W. Barry
	AVCO Corporation, Government Products Group, 201 Lowell Street, Wilmington, Massachusetts 01997
1	ATTN: Dr. W. Reinecke
1	Mr. P. Rolincik
	Battelle Columbus Laboratories, 505 King Avenue, Columbus, Ohio 43201
1	ATTN: Mr. J. Mueller
	Brush Wellman Corporation, 17676 St. Clair Avenue, Cleveland, Ohio 44114
1	ATTN: Mr. J. Stonehouse
	Effects Technology, Inc., 5383 Hollister Avenue, Santa Barbara, California 93111
1	ATTN: Dr. R. Wengler
1	Dr. R. Parisse
1	Mr. J. Green
	ETA Corporation, P. O. Box 6625, Orange, California 92667
1	ATTN: Mr. D. L. Mykkanen

No. of Copies	To
1	Fiber Materials, Inc., Biddeford Industrial Park, Biddeford, Maine 04005
1	ATTN: Mr. M. Subilia, Jr.
1	Mr. L. Landers
1	Mr. G. Williams
1	Mr. P. Marchol
	General Dynamics Corporation, Convair Division, 5001 Kearny Villa Road, San Diego, California 92138
1	ATTN: J. Hertz
1	H. McCutcheon, Jr.
	General Electric Company, Valley Forge Space Technology Center, P. O. Box 8555, Philadelphia, Pennsylvania 19101
1	ATTN: K. Hall
1	J. Brazel
1	Ms. B. McGuire
	Kaman Sciences Corporation, P. O. Box 7463, Colorado Springs, Colorado 80933
1	ATTN: F. Shelton
	Kawecki Berylco Industries, Inc., P. O. Box 1462, Reading, Pennsylvania 19603
1	ATTN: Norman P. Pinto
	Ktech, 911 Pennsylvania Avenue, N.E., Albuquerque, New Mexico 87110
1	ATTN: Dr. D. Keller
	Lawrence Livermore Laboratory, P. O. Box 808, Livermore, California 94550
1	ATTN: Lee Roberts
1	James E. Hanafee
	Lehigh University, Institute of Fracture and Solid Mechanics, Packard Lab., Bldg. 19, Bethlehem, Pennsylvania 18015
1	ATTN: Dr. G. C. Sih
	Lockheed Missiles and Space Company, P. O. Box 504, Sunnyvale, California 94088
1	ATTN: D. Aspinwall
1	Mr. M. V. Rebholz
	Lockheed Palo Alto Research Laboratory, 3251 Hanover Street, Palo Alto, California 94304
1	ATTN: Mr. D. Webster
	Los Alamos Scientific Laboratory, P. O. Box 1663, Los Alamos, New Mexico 87544
1	ATTN: GMX-6, Dr. J. W. Taylor
1	Mr. J. E. Hockett

No. of Copies	To
	Martin Marietta Corporation, P. O. Box 5837, Orlando, Florida 32805
1	ATTN: Dr. M. Hendricks
1	R. Hewitt
1	Mr. F. H. Koo
	McDonnel Douglas Corporation, 5301 Bolsa Avenue, Huntington Beach, California 92647
1	ATTN: Dr. L. Cohen
1	H. Parachanian
	Prototype Development Associates, Inc., 1740 Garry Avenue, Suite 201 Santa Ana, California 92705
1	ATTN: J. Schultzler
1	N. Harrington
	R&D Associates, 525 Wilshire Boulevard, Santa Monica, California 90025
1	ATTN: Dr. A. Field
	Radkowski Associates, P. O. Box 5474, Riverside, California 92507
1	ATTN: Dr. P. Radkowski
	Rockwell International, Rocky Flats Plant, P. O. Box 464, Golden, Colorado 80401
1	ATTN: S. Beitscher
	S. H. Gelles Associates, 2840 Fisher Road, Columbus, Ohio 43204
1	ATTN: S. H. Gelles
	Sandia Laboratories, P. O. Box 5800, Albuquerque, New Mexico 87115
1	ATTN: Dr. W. Herrmann
1	Dr. L. D. Bertholf
1	Dr. J. Lipkin
	Sandia Laboratories, Livermore, California 94550
1	ATTN: Donald R. Adolphson
1	J. E. Smugeresky
1	B. C. Odegard
	Southwest Research Institute, 8500 Culebra Road, San Antonio, Texas 78206
1	ATTN: Mr. A. Wenzel
	Stanford Research Institute, 333 Ravenswood Avenue, Menlo Park, California 90250
1	ATTN: Dr. D. Curran
1	Dr. L. Seaman
	Stanford University, Department of Applied Mechanics, Stanford, California 94305
1	ATTN: Prof. E. H. Lee
	TRW Systems Group, One Space Park, Redondo Beach, California 90278
1	ATTN: D. Gamble
	Director, Army Materials and Mechanics Research Center, Watertown, Massachusetts 02172
1	ATTN: DRXMR-PL
1	DRXMR-WD
3	Authors

Army Materials and Mechanics Research Center, Watertown, Massachusetts 02172
CHARACTERISTICS OF MECHANICALLY FASTENED JOINTS OF CIP/HIP-1 BERYLLIUM - Shun-Chin Chou, James H. Rainey, and Ronald A. Swanson

Technical Report AMMRC TR 79-48, August 1979, 31 pp - illus-tables, D/A Project 8X3633304D215 AMCMS Code 633304.21500.03

AD___________________

UNCLASSIFIED
UNLIMITED DISTRIBUTION

Key Words

Beryllium
Bearing strength
Loading rate

Mechanically fastened joints of CIP/HIP-1 beryllium were investigated. A standard ASTM pin-jointed bearing strength test was used to determine the effect of hole size and edge distance-to-thickness ratios on the bearing strength of beryllium plates. Joints for structures were studied by testing two types of arrangements of pin holes with different t ınsverse pitches. From the standard ASTM pin-jointed bearing strength tests, it was determined that the design criterion for single-pinned joints of CIP/HIP-1 beryllium should be based on maximum stress instead of net cross-section stress. Furthermore, it was found that if the edge distance-to-pin diameter ratio was kept constant, the specimens would have the same bearing yield stress, bearing strength, and maximum bearing strain. In the investigation of structural bolted joints, the double-bolted joints show that the transverse pitch and hole pattern have no effect on the load-carrying capability.

Army Materials and Mechanics Research Center, Watertown, Massachusetts 02172
CHARACTERISTICS OF MECHANICALLY FASTENED JOINTS OF CIP/HIP-1 BERYLLIUM - Shun-Chin Chou, James H. Rainey, and Ronald A. Swanson

Technical Report AMMRC TR 79-48, August 1979, 31 pp - illus-tables, D/A Project 8X3633304D215 AMCMS Code 633304.21500.03

AD___________________

UNCLASSIFIED
UNLIMITED DISTRIBUTION

Key Words

Beryllium
Bearing strength
Loading rate

Mechanically fastened joints of CIP/HIP-1 beryllium were investigated. A standard ASTM pin-jointed bearing strength test was used to determine the effect of hole size and edge distance-to-thickness ratios on the bearing strength of beryllium plates. Joints for structures were studied by testing two types of arrangements of pin holes with different transverse pitches. From the standard ASTM pin-jointed bearing strength tests, it was determined that the design criterion for single-pinned joints of CIP/HIP-1 beryllium should be based on maximum stress instead of net cross-section stress. Furthermore, it was found that if the edge distance-to-pin diameter ratio was kept constant, the specimens would have the same bearing yield stress, bearing strength, and maximum bearing strain. In the investigation of structural bolted joints, the double-bolted joints show that the transverse pitch and hole pattern have no effect on the load-carrying capability.

Army Materials and Mechanics Research Center, Watertown, Massachusetts 02172
CHARACTERISTICS OF MECHANICALLY FASTENED JOINTS OF CIP/HIP-1 BERYLLIUM - Shun-Chin Chou, James H. Rainey, and Ronald A. Swanson

Technical Report AMMRC TR 79-48, August 1979, 31 pp - illus-tables, D/A Project 8X3633304D215 AMCMS Code 633304.21500.03

AD___________________

UNCLASSIFIED
UNLIMITED DISTRIBUTION

Key Words

Beryllium
Bearing strength
Loading rate

Mechanically fastened joints of CIP/HIP-1 beryllium were investigated. A standard ASTM pin-jointed bearing strength test was used to determine the effect of hole size and edge distance-to-thickness ratios on the bearing strength of beryllium plates. Joints for structures were studied by testing two types of arrangements of pin holes with different transverse pitches. From the standard ASTM pin-jointed bearing strength tests, it was determined that the design criterion for single-pinned joints of CIP/HIP-1 beryllium should be based on maximum stress instead of net cross-section stress. Furthermore, it was found that if the edge distance-to-pin diameter ratio was kept constant, the specimens would have the same bearing yield stress, bearing strength, and maximum bearing strain. In the investigation of structural bolted joints, the double-bolted joints show that the transverse pitch and hole pattern have no effect on the load-carrying capability.

Army Materials and Mechanics Research Center, Watertown, Massachusetts 02172
CHARACTERISTICS OF MECHANICALLY FASTENED JOINTS OF CIP/HIP-1 BERYLLIUM - Shun-Chin Chou, James H. Rainey, and Ronald A. Swanson

Technical Report AMMRC TR 79-48, August 1979, 31 pp - illus-tables, D/A Project 8X3633304D215 AMCMS Code 633304.21500.03

AD___________________

UNCLASSIFIED
UNLIMITED DISTRIBUTION

Key Words

Beryllium
Bearing strength
Loading rate

Mechanically fastened joints of CIP/HIP-1 beryllium were investigated. A standard ASTM pin-jointed bearing strength test was used to determine the effect of hole size and edge distance-to-thickness ratios on the bearing strength of beryllium plates. Joints for structures were studied by testing two types of arrangements of pin holes with different transverse pitches. From the standard ASTM pin-jointed bearing strength tests, it was determined that the design criterion for single-pinned joints of CIP/HIP-1 beryllium should be based on maximum stress instead of net cross-section stress. Furthermore, it was found that if the edge distance-to-pin diameter ratio was kept constant, the specimens would have the same bearing yield stress, bearing strength, and maximum bearing strain. In the investigation of structural bolted joints, the double-bolted joints show that the transverse pitch and hole pattern have no effect on the load-carrying capability.